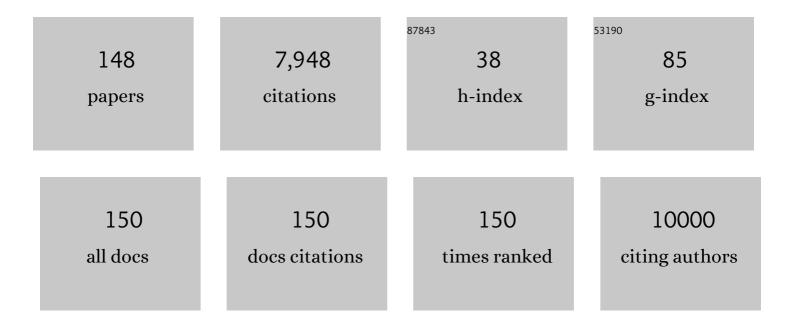
Richard B Thompson

List of Publications by Year in descending order

Source: https://exaly.com/author-pdf/8769666/publications.pdf Version: 2024-02-01



#	Article	lF	CITATIONS
1	Cardiac and cardiometabolic phenotyping of trastuzumab-mediated cardiotoxicity: a secondary analysis of the MANTICORE trial. European Heart Journal - Cardiovascular Pharmacotherapy, 2022, 8, 130-139.	1.4	24
2	Impaired Muscle Oxygen Extraction Kinetics in Cirrhosis: Muscle Is a Major Contributor to Impaired Wholeâ€Body Exercise Capacity. Liver Transplantation, 2022, 28, 321-324.	1.3	0
3	Remote ischaemic conditioning in ST elevation myocardial infarction: a registry-based randomised trial. Heart, 2022, 108, 703-709.	1.2	2
4	Improved accuracy and precision with threeâ€parameter simultaneous myocardial T ₁ and T ₂ mapping using multiparametric SASHA. Magnetic Resonance in Medicine, 2022, 87, 2775-2791.	1.9	13
5	A Contemporary Review of the Effects of Exercise Training on Cardiac Structure and Function and Cardiovascular Risk Profile: Insights From Imaging. Frontiers in Cardiovascular Medicine, 2022, 9, 753652.	1.1	4
6	Decongestive progressive resistance exercise with an adjustable compression wrap for breast cancer-related lymphoedema (DREAM): protocol for a randomised controlled trial. BMJ Open, 2022, 12, e053165.	0.8	0
7	Longitudinal Changes in Skeletal Muscle Metabolism, Oxygen Uptake, and Myosteatosis During Cardiotoxic Treatment for Early-Stage Breast Cancer. Oncologist, 2022, 27, e748-e754.	1.9	9
8	Demystifying Cardiac Iron Deficiency in Endâ€stage Heart Failure. FASEB Journal, 2022, 36, .	0.2	0
9	Time-Restricted Eating to Reduce Cardiovascular Risk Among Older Breast Cancer Survivors. JACC: CardioOncology, 2022, 4, 276-278.	1.7	7
10	Myocardial Iron Deficiency and Mitochondrial Dysfunction in Advanced Heart Failure in Humans. Journal of the American Heart Association, 2022, 11, .	1.6	22
11	Quantification of changes in myocardial <scp>T₁</scp> * values with exercise cardiac <scp>MRI</scp> using a freeâ€breathing <scp>nonâ€electrocardiograph</scp> radial imaging. Magnetic Resonance in Medicine, 2022, 88, 1720-1733.	1.9	2
12	Left atrial remodelling, mid-regional pro-atrial natriuretic peptide, and prognosis across a range of ejection fractions in heart failure. European Heart Journal Cardiovascular Imaging, 2021, 22, 220-228.	0.5	10
13	Simultaneous pro ton density f atâ€fraction and i maging with waterâ€specific T₁ mapping (PROFIT ₁): application in liver. Magnetic Resonance in Medicine, 2021, 85, 223-238.	1.9	20
14	Freeâ€breathing simultaneous myocardial T ₁ and T ₂ mapping with whole left ventricle coverage. Magnetic Resonance in Medicine, 2021, 85, 1308-1321.	1.9	16
15	Reliability and reproducibility of cardiac MRI quantification of peak exercise function with long-axis views. PLoS ONE, 2021, 16, e0245912.	1.1	7
16	Quantification of lung water density with UTE Yarnball MRI. Magnetic Resonance in Medicine, 2021, 86, 1330-1344.	1.9	8
17	Tricuspid Valve Tethering Is Associated with Residual Regurgitation after Valve Repair in Hypoplastic Left Heart Syndrome: A Three-Dimensional Echocardiographic Study. Journal of the American Society of Echocardiography, 2021, 34, 1199-1210.	1.2	10
18	Cardiac and skeletal muscle predictors of impaired cardiorespiratory fitness post-anthracycline chemotherapy for breast cancer. Scientific Reports, 2021, 11, 14005.	1.6	11

#	Article	IF	CITATIONS
19	Cardiac remodelling predicts outcome in patients with chronic heart failure. ESC Heart Failure, 2021, 8, 5352-5362.	1.4	12
20	Aerobic Fitness Is Related to Myocardial Fibrosis Post–Anthracycline Therapy. Medicine and Science in Sports and Exercise, 2021, 53, 267-274.	0.2	7
21	Rationale and design of the Diet Restriction and Exercise-induced Adaptations in Metastatic breast cancer (DREAM) study: a 2-arm, parallel-group, phase II, randomized control trial of a short-term, calorie-restricted, and ketogenic diet plus exercise during intravenous chemotherapy versus usual care. BMC Cancer, 2021, 21, 1093.	1.1	19
22	Tilt-table Echocardiography Unmasks Early Diastolic Dysfunction in Patients With Hemoglobinopathies. Journal of Pediatric Hematology/Oncology, 2020, 42, 391-397.	0.3	5
23	Layer-specific strain in patients with heart failure using cardiovascular magnetic resonance: not all layers are the same. Journal of Cardiovascular Magnetic Resonance, 2020, 22, 81.	1.6	21
24	Circulating troponin and further left ventricular ejection fraction improvement in patients with previously recovered left ventricular ejection fraction. ESC Heart Failure, 2020, 7, 2725-2733.	1.4	7
25	Exercise Intolerance in Anthracycline-Treated Breast Cancer Survivors: The Role of Skeletal Muscle Bioenergetics, Oxygenation, and Composition. Oncologist, 2020, 25, e852-e860.	1.9	25
26	A Novel Right Ventricular Volume and Pressure Loaded Piglet Heart Model for the Study of Tricuspid Valve Function Journal of Visualized Experiments, 2020, , .	0.2	2
27	Measurement and correction of the bulk magnetic susceptibility effects of fat: application in venous oxygen saturation imaging. Magnetic Resonance in Medicine, 2019, 81, 3124-3137.	1.9	4
28	Quantification of lung water in heart failure using cardiovascular magnetic resonanceÂimaging. Journal of Cardiovascular Magnetic Resonance, 2019, 21, 58.	1.6	14
29	The Effect of Blood Composition on T1ÂMapping. JACC: Cardiovascular Imaging, 2019, 12, 1888-1890.	2.3	9
30	A cardiac magnetic resonance imaging study of long-term and incident hemodialysis patients. Journal of Nephrology, 2019, 32, 615-626.	0.9	5
31	Myocardial native T1 and extracellular volume with healthy ageing and gender. European Heart Journal Cardiovascular Imaging, 2018, 19, 615-621.	0.5	78
32	Simulation-based quantification of native T1 and T2 of the myocardium using a modified MOLLI scheme and the importance of Magnetization Transfer. Magnetic Resonance Imaging, 2018, 48, 96-106.	1.0	12
33	Home Exercise Training Improves Exercise Capacity in Cirrhosis Patients: Role of Exercise Adherence. Scientific Reports, 2018, 8, 99.	1.6	89
34	Tricuspid Valve Adaptation during the First Interstage Period in Hypoplastic Left Heart Syndrome. Journal of the American Society of Echocardiography, 2018, 31, 624-633.	1.2	16
35	Comparison of Cardiac Magnetic Resonance Imaging and Echocardiography in Assessment of Left Ventricular Hypertrophy in Fabry Disease. Canadian Journal of Cardiology, 2018, 34, 1041-1047.	0.8	19
36	Effects of age, gender, and risk-factors for heart failure on native myocardial T1 and extracellular volume fraction using the SASHA sequence at 1.5T. Journal of Magnetic Resonance Imaging, 2018, 48, spcone-spcone.	1.9	0

#	Article	IF	CITATIONS
37	Rationale and design of the Caloric Restriction and Exercise protection from Anthracycline Toxic Effects (CREATE) study: a 3-arm parallel group phase II randomized controlled trial in early breast cancer. BMC Cancer, 2018, 18, 864.	1.1	22
38	Effects of age, gender, and riskâ€factors for heart failure on native myocardial T ₁ and extracellular volume fraction using the SASHA sequence at 1.5T. Journal of Magnetic Resonance Imaging, 2018, 48, 1307-1317.	1.9	9
39	Characterization of T ₁ bias in skeletal muscle from fat in MOLLI and SASHA pulse sequences: Quantitative fatâ€fraction imaging with T ₁ mapping. Magnetic Resonance in Medicine, 2017, 77, 237-249.	1.9	25
40	Clinical Features, Diagnosis, and Management of Patients With Anderson-Fabry Cardiomyopathy. Canadian Journal of Cardiology, 2017, 33, 883-897.	0.8	34
41	Increased left ventricular extracellular volume and enhanced twist function in type 1 diabetic individuals. Journal of Applied Physiology, 2017, 123, 394-401.	1.2	19
42	Myocardial tissue deformation is reduced in subjects with coronary microvascular dysfunction but not rescued by treatment with ranolazine. Clinical Cardiology, 2017, 40, 300-306.	0.7	22
43	Multidisciplinary Approach to Novel Therapies in Cardio-Oncology Research (MANTICORE 101–Breast): A Randomized Trial for the Prevention of Trastuzumab-Associated Cardiotoxicity. Journal of Clinical Oncology, 2017, 35, 870-877.	0.8	292
44	Inhibition of pyruvate dehydrogenase kinase improves pulmonary arterial hypertension in genetically susceptible patients. Science Translational Medicine, 2017, 9, .	5.8	206
45	Subclinical Pulmonary Edema Is Associated With Reduced Exercise Capacity in HFpEF and HFrEF. Journal of the American College of Cardiology, 2017, 70, 1827-1828.	1.2	11
46	Clinical recommendations for cardiovascular magnetic resonance mapping of T1, T2, T2* and extracellular volume: A consensus statement by the Society for Cardiovascular Magnetic Resonance (SCMR) endorsed by the European Association for Cardiovascular Imaging (EACVI). Journal of Cardiovascular Magnetic Resonance, 2017, 19, 75.	1.6	1,074
47	Differential Responses of Post-Exercise Recovery of Leg Blood Flow and Oxygen Uptake Kinetics in HFpEF versus HFrEF. PLoS ONE, 2016, 11, e0163513.	1.1	11
48	Altered breathing mechanics and ventilatory response during exercise in children born extremely preterm. Thorax, 2016, 71, 1012-1019.	2.7	53
49	Impaired Left Ventricular Reserve in Childhood Cancer Survivors Treated With Anthracycline Therapy. Pediatric Blood and Cancer, 2016, 63, 1086-1090.	0.8	19
50	Evaluation of Cardiac, Vascular, and Skeletal Muscle Function With MRI: Novel Physiological End Points in Cardiac Rehabilitation Research. Canadian Journal of Cardiology, 2016, 32, S388-S396.	0.8	7
51	Quantification of pulmonary edema in heart failure using MRI: invasive validation and evaluation in HFpEF and HFrEF patients. Journal of Cardiovascular Magnetic Resonance, 2016, 18, O49.	1.6	1
52	Differential responses of post-exercise recovery leg blood flow and oxygen uptake kinetics in HFPEF versus HFREF. Journal of Cardiovascular Magnetic Resonance, 2016, 18, O9.	1.6	1
53	An index for diagnosing infant hip dysplasia using 3-D ultrasound: the acetabular contact angle. Pediatric Radiology, 2016, 46, 1023-1031.	1.1	18
54	Reduced Right Ventricular Native Myocardial T1 in Anderson-Fabry Disease: Comparison to Pulmonary Hypertension and Healthy Controls. PLoS ONE, 2016, 11, e0157565.	1.1	30

RICHARD B THOMPSON

#	Article	IF	CITATIONS
55	Saturation pulse design for quantitative myocardial T1 mapping. Journal of Cardiovascular Magnetic Resonance, 2015, 17, 84.	1.6	31
56	Variability of T1 in purpose recruited normal volunteers and patients as a function of shim (B0), flip angle (B1) and myocardial sector at 3T. Journal of Cardiovascular Magnetic Resonance, 2015, 17, P5.	1.6	3
57	Genderâ€specific plasma proteomic biomarkers in patients with Anderson–Fabry disease. European Journal of Heart Failure, 2015, 17, 291-300.	2.9	38
58	Feasibility and reproducibility of measurement of whole muscle blood flow, oxygen extraction, and VO ₂ with dynamic exercise using MRI. Magnetic Resonance in Medicine, 2015, 74, 1640-1651.	1.9	16
59	Correlation of cardiovascular magnetic resonance imaging findings and endomyocardial biopsy results in patients undergoing screening for heart transplant rejection. Journal of Heart and Lung Transplantation, 2015, 34, 643-650.	0.3	77
60	Characterization of T1 bias from lipids in MOLLI and SASHA pulse sequences. Journal of Cardiovascular Magnetic Resonance, 2015, 17, .	1.6	6
61	Optimized saturation pulse rrains for SASHA T1 mapping at 3T. Journal of Cardiovascular Magnetic Resonance, 2015, 17, W20.	1.6	3
62	Normal left-atrial structure and function despite concentric left-ventricular remodelling in a cohort of patients with Anderson–Fabry disease. European Heart Journal Cardiovascular Imaging, 2015, 16, 1129-1136.	0.5	9
63	Reproducibility of Acetabular Landmarks and a Standardized Coordinate System Obtained from 3D Hip Ultrasound. Ultrasonic Imaging, 2015, 37, 267-276.	1.4	13
64	Ultrasound Quantification of Acetabular Rounding in Hip Dysplasia: Reliability and Correlation to Treatment Decisions in a Retrospective Study. Ultrasound in Medicine and Biology, 2015, 41, 56-63.	0.7	7
65	Quantification of circumferential, longitudinal, and radial global fractional shortening using steadyâ€state free precession cines: A comparison with tissueâ€tracking strain and application in fabry disease. Magnetic Resonance in Medicine, 2015, 73, 586-596.	1.9	12
66	Anderson-Fabry cardiomyopathy: prevalence, pathophysiology, diagnosis and treatment. Heart Failure Reviews, 2015, 20, 179-191.	1.7	58
67	Reliability of 3D localisation of ACL attachments on MRI: comparison using multi-planar 2D versus high-resolution 3D base sequences. Knee Surgery, Sports Traumatology, Arthroscopy, 2015, 23, 1206-1214.	2.3	14
68	Real-Time Visualization of Joint Cavitation. PLoS ONE, 2015, 10, e0119470.	1.1	46
69	Tricuspid Regurgitation in Hypoplastic Left Heart Syndrome. Circulation: Cardiovascular Imaging, 2014, 7, 765-772.	1.3	58
70	Potential for Change in US Diagnosis of Hip Dysplasia Solely Caused by Changes in Probe Orientation: Patterns of Alpha-angle Variation Revealed by Using Three-dimensional US. Radiology, 2014, 273, 870-878.	3.6	59
71	Accuracy, Precision, and Reproducibility of Four T1 Mapping Sequences: A Head-to-Head Comparison of MOLLI, ShMOLLI, SASHA, and SAPPHIRE. Radiology, 2014, 272, 683-689.	3.6	255
72	Velocity encoding with the slice select refocusing gradient for faster imaging and reduced chemical shiftâ€induced phase errors. Magnetic Resonance in Medicine, 2014, 71, 2014-2023.	1.9	4

RICHARD B THOMPSON

#	Article	IF	CITATIONS
73	Saturation recovery singleâ€ s hot acquisition (SASHA) for myocardial <i>T</i> ₁ mapping. Magnetic Resonance in Medicine, 2014, 71, 2082-2095.	1.9	307
74	The Alberta Heart Failure Etiology and Analysis Research Team (HEART) study. BMC Cardiovascular Disorders, 2014, 14, 91.	0.7	27
75	Improved precision in SASHA T1 mapping with a variable flip angle readout. Journal of Cardiovascular Magnetic Resonance, 2014, 16, M9.	1.6	16
76	Optimized saturation recovery protocols for T1-mapping in the heart: influence of sampling strategies on precision. Journal of Cardiovascular Magnetic Resonance, 2014, 16, 55.	1.6	42
77	Diffuse myocardial fibrosis by T1-mapping in children with subclinical anthracycline cardiotoxicity: relationship to exercise capacity, cumulative dose and remodeling. Journal of Cardiovascular Magnetic Resonance, 2013, 15, 48.	1.6	189
78	Systolic and Diastolic Function Assessment in Fabry Disease Patients Using Speckle-Tracking Imaging and Comparison with Conventional Echocardiographic Measurements. Journal of the American Society of Echocardiography, 2013, 26, 1407-1414.	1.2	72
79	Myocardial Deformation Analysis in Contrast Echocardiography: First Results Using Two-Dimensional Cardiac Performance Analysis. Journal of the American Society of Echocardiography, 2013, 26, 1282-1289.	1.2	7
80	Late Gadolinium Enhancement in Cardiac Transplant Patients Is Associated With Adverse Ventricular Functional Parameters and Clinical Outcomes. Canadian Journal of Cardiology, 2013, 29, 1076-1083.	0.8	22
81	Prevention of deep tissue injury through muscle contractions induced by intermittent electrical stimulation after spinal cord injury in pigs. Journal of Applied Physiology, 2013, 114, 286-296.	1.2	12
82	T ₁ Mapping With Cardiovascular MRI Is Highly Sensitive for Fabry Disease Independent of Hypertrophy and Sex. Circulation: Cardiovascular Imaging, 2013, 6, 637-645.	1.3	158
83	Reliability of Estimates of ACL Attachment Locations in 3-Dimensional Knee Reconstruction Based on Routine Clinical MRI in Pediatric Patients. American Journal of Sports Medicine, 2013, 41, 1319-1329.	1.9	11
84	Quantitative Real-Time Three-Dimensional Echocardiography Provides New Insight into the Mechanisms of Mitral Valve Regurgitation Post-Repair of Atrioventricular Septal Defect. Journal of the American Society of Echocardiography, 2012, 25, 1231-1244.	1.2	39
85	Transport Phenomena in Articular Cartilage Cryopreservation as Predicted by the Modified Triphasic Model and the Effect of Natural Inhomogeneities. Biophysical Journal, 2012, 102, 1284-1293.	0.2	32
86	Enhancement of spectral editing efficacy of multiple quantum filters in in vivo proton magnetic resonance spectroscopy. Journal of Magnetic Resonance, 2012, 223, 90-97.	1.2	3
87	MR spectroscopy measurement of the diffusion of dimethyl sulfoxide in articular cartilage and comparison to theoretical predictions. Osteoarthritis and Cartilage, 2012, 20, 1004-1010.	0.6	24
88	T2-dependent errors in MOLLI T1 values: simulations, phantoms, and in-vivo studies. Journal of Cardiovascular Magnetic Resonance, 2012, 14, .	1.6	28
89	Using MRI to Measure Aerosol Deposition. Journal of Aerosol Medicine and Pulmonary Drug Delivery, 2012, 25, 55-62.	0.7	30
90	Heart failure with preserved ejection fraction in the elderly: scope of the problem. Heart Failure Reviews, 2012, 17, 555-562.	1.7	38

6

#	Article	IF	CITATIONS
91	Distribution of Internal Pressure around Bony Prominences: Implications to Deep Tissue Injury and Effectiveness of Intermittent Electrical Stimulation. Annals of Biomedical Engineering, 2012, 40, 1740-1759.	1.3	22
92	Distribution of Internal Strains Around Bony Prominences in Pigs. Annals of Biomedical Engineering, 2012, 40, 1721-1739.	1.3	10
93	Intermittent electrical stimulation redistributes pressure and promotes tissue oxygenation in loaded muscles of individuals with spinal cord injury. Journal of Applied Physiology, 2011, 110, 246-255.	1.2	36
94	Effects of Intermittent Electrical Stimulation on Superficial Pressure, Tissue Oxygenation, and Discomfort Levels for the Prevention of Deep Tissue Injury. Annals of Biomedical Engineering, 2011, 39, 649-663.	1.3	27
95	Rationale and design of the Multidisciplinary Approach to Novel Therapies in Cardiology Oncology Research Trial (MANTICORE 101 - Breast): a randomized, placebo-controlled trial to determine if conventional heart failure pharmacotherapy can prevent trastuzumab-mediated left ventricular remodeling among patients with HER2+ early breast cancer using cardiac MRI. BMC Cancer, 2011, 11, 318.	1.1	76
96	Degree of diffuse fibrosis measured by MRI correlates with LV remodelling in childhood cancer survivors after anthracycline chemotherapy. Journal of Cardiovascular Magnetic Resonance, 2011, 13, .	1.6	9
97	Characterization of myocardial T1 and partition coefficient as a function of time after gadolinium delivery in healthy subjects. Journal of Cardiovascular Magnetic Resonance, 2011, 13, .	1.6	2
98	Triplanar estimation of left atrial volume. Journal of Cardiovascular Magnetic Resonance, 2011, 13, .	1.6	1
99	Effect of acute high-intensity interval exercise on postexercise biventricular function in mild heart failure. Journal of Applied Physiology, 2011, 110, 398-406.	1.2	26
100	Left ventricular systolic and diastolic function during tilt-table positioning and passive heat stress in humans. American Journal of Physiology - Heart and Circulatory Physiology, 2011, 301, H599-H608.	1.5	30
101	Pilot Study of Inhaled Aerosols Targeted via Magnetic Alignment of High Aspect Ratio Particles in Rabbits. Journal of Nanomaterials, 2011, 2011, 1-7.	1.5	8
102	Left ventricular systolic and diastolic function during orthostatic heat stress. FASEB Journal, 2011, 25, 1053.2.	0.2	0
103	Changes in ventricular twist and untwisting with orthostatic stress: endurance athletes versus normally active individuals. Journal of Applied Physiology, 2010, 108, 1259-1266.	1.2	19
104	Effects of High Intensity Exercise on Biventricular Function Assessed by Cardiac Magnetic Resonance Imaging in Endurance Trained and Normally Active Individuals. American Journal of Cardiology, 2010, 106, 278-283.	0.7	19
105	Difference spectroscopy using PRESS asymmetry: application to glutamate, glutamine, and myo-inositol. NMR in Biomedicine, 2010, 23, 41-47.	1.6	9
106	Characterization of the relationship between systolic shear strain and early diastolic shear strain rates: insights into torsional recoil. American Journal of Physiology - Heart and Circulatory Physiology, 2010, 299, H898-H907.	1.5	23
107	Increased left ventricular twist, untwisting rates, and suction maintain global diastolic function during passive heat stress in humans. American Journal of Physiology - Heart and Circulatory Physiology, 2010, 298, H930-H937.	1.5	47
108	Measurements of changes in left ventricular volume, strain, and twist during isovolumic relaxation using MRI. American Journal of Physiology - Heart and Circulatory Physiology, 2010, 298, H1908-H1918.	1.5	20

RICHARD B THOMPSON

#	Article	IF	CITATIONS
109	Aerobic fitness does not influence the biventricular response to whole body passive heat stress. Journal of Applied Physiology, 2010, 109, 1545-1551.	1.2	9
110	Normal Rotational, Torsion and Untwisting Data in Children, Adolescents and Young Adults. Journal of the American Society of Echocardiography, 2010, 23, 286-293.	1.2	63
111	Deposition of Inhaled Ultrafine Aerosols in Replicas of Nasal Airways of Infants. Aerosol Science and Technology, 2010, 44, 741-752.	1.5	31
112	Clobal diastolic function is preserved during passive heat stress due to augmented left ventricular untwisting. FASEB Journal, 2010, 24, 991.20.	0.2	0
113	Real-Time 3-Dimensional Echocardiography Provides New Insight Into Mechanisms of Tricuspid Valve Regurgitation in Patients With Hypoplastic Left Heart Syndrome. Circulation, 2009, 120, 1091-1098.	1.6	88
114	Cardiovascular responses to incremental and sustained submaximal exercise in heart transplant recipients. American Journal of Physiology - Heart and Circulatory Physiology, 2009, 296, H350-H358.	1.5	26
115	Adjuvant Trastuzumab Induces Ventricular Remodeling Despite Aerobic Exercise Training. Clinical Cancer Research, 2009, 15, 4963-4967.	3.2	111
116	Contamination of singleâ€voxel multiple quantum filters by external water signals arising from intermolecular multiple quantum coherences. Magnetic Resonance in Medicine, 2009, 62, 796-801.	1.9	3
117	Cardiovascular magnetic resonance in the diagnosis of acute heart transplant rejection: a review. Journal of Cardiovascular Magnetic Resonance, 2009, 11, 7.	1.6	79
118	Left ventricular torsion and untwisting during exercise in heart transplant recipients. Journal of Physiology, 2009, 587, 2375-2386.	1.3	44
119	1135 Exploring pressure gradients measured in the left heart during diastole. Journal of Cardiovascular Magnetic Resonance, 2008, 10, .	1.6	0
120	Freeâ€breathing cine MRI. Magnetic Resonance in Medicine, 2008, 60, 709-717.	1.9	21
121	Strongly coupled versus uncoupled spin response to radio frequency interference effects: application to glutamate and glutamine in spectroscopic imaging. NMR in Biomedicine, 2008, 21, 402-409.	1.6	5
122	MRI Measurement of Regional Lung Deposition in Mice Exposed Nose-Only to Nebulized Superparamagnetic Iron Oxide Nanoparticles. Journal of Aerosol Medicine and Pulmonary Drug Delivery, 2008, 21, 335-342.	0.7	41
123	Prevention of pressure-induced deep tissue injury using intermittent electrical stimulation. Journal of Applied Physiology, 2007, 102, 1992-2001.	1.2	35
124	Accuracy and reliability of MRI vs. laboratory measurements in an ex vivo porcine model of arthritic cartilage loss. Journal of Magnetic Resonance Imaging, 2007, 26, 992-1000.	1.9	6
125	A Mitochondria-K+ Channel Axis Is Suppressed in Cancer and Its Normalization Promotes Apoptosis and Inhibits Cancer Growth. Cancer Cell, 2007, 11, 37-51.	7.7	1,374
126	Partial field-of-view spiral phase-contrast imaging using complex difference processing. Magnetic Resonance in Medicine, 2006, 56, 676-680.	1.9	3

ARTICLE IF CITATIONS Cardiorespiratory-resolved magnetic resonance imaging: Measuring respiratory modulation of cardiac function. Magnetic Resonance in Medicine, 2006, 56, 1301-1310. Image Based Temporal Registration of MRI Data for Medical Visualization., 2006,,. 128 8 Variability of metabolite yield using STEAM or PRESS sequences in vivo at 3.0 T, illustrated with 129 28 myo-inositol. Magnetic Resonance in Medicine, 2005, 53, 760-769. Measurement of skeletal muscle perfusion during postischemic reactive hyperemia using 130 1.9 57 contrast-enhanced MRI with a step-input function. Magnetic Resonance in Medicine, 2005, 54, 289-298. Invasive human magnetic resonance imaging: Feasibility during revascularization in a combined XMR 56 suite. Catheterization and Cardiovascular Interventions, 2005, 64, 265-274. Real-Time Magnetic Resonance Imaging–Guided Stenting of Aortic Coarctation With Commercially Available Catheter Devices in Swine. Circulation, 2005, 112, 699-706. 132 82 1.6 Real-Time Magnetic Resonance-Guided Endovascular Repair of Experimental Abdominal Aortic 1.2 61 Aneurysm in Šwine. Journal of the American College of Cardiology, 2005, 45, 2069-2077. Flow-gated phase-contrast MRI using radial acquisitions. Magnetic Resonance in Medicine, 2004, 52, 134 1.9 42 598-604. Serial Cardiac Magnetic Resonance Imaging of Injected Mesenchymal Stem Cells. Circulation, 2003, 108, 1.6 1009-1014. Fast measurement of intracardiac pressure differences with 2D breath-hold phase-contrast MRI. 136 1.9 63 Magnetic Resonance in Medicine, 2003, 49, 1056-1066. Real-time volumetric flow measurements with complex-difference MRI. Magnetic Resonance in 1.9 Medicine, 2003, 50, 1248-1255. Catheter-Based Endomyocardial Injection With Real-Time Magnetic Resonance Imaging. Circulation, 138 1.6 134 2002, 105, 1282-1284. High temporal resolution phase contrast MRI with multiecho acquisitions. Magnetic Resonance in 1.9 Medicine, 2002, 47, 499-512. Catheter-based endomyocardial injection with real-time magnetic resonance imaging. Circulation, 140 1.6 65 2002, 105, 1282-4. Response of metabolites with coupled spins to the STEAM sequence. Magnetic Resonance in Medicine, 141 2001, 45, 955-965. Response of metabolites with coupled spins to the STEAM sequence. Magnetic Resonance in Medicine, 142 1.9 1 2001, 45, 955-965. On the localized quantification of metabolites with coupled spins. Magnetic Resonance Materials in 1.1 Physics, Biology, and Medicine, 1999, 9, 159-163. Sources of variability in the response of coupled spins to the PRESS sequence and their potential 144 1.9 88 impact on metabolite quantification. Magnetic Resonance in Medicine, 1999, 41, 1162-1169.

RICHARD B THOMPSON

44

#	Article	IF	CITATIONS
145	Residual dipolar coupling of the Cr/PCr methyl resonance in resting human medial gastrocnemius muscle. Magnetic Resonance in Medicine, 1999, 42, 421-424.	1.9	30
146	A new multiple quantum filter design procedure for use on strongly coupled spin systems foundin vivo: Its application to glutamate. Magnetic Resonance in Medicine, 1998, 39, 762-771.	1.9	71
147	The role of the <i>N</i> -acetylaspartate multiplet in the quantification of brain metabolites. Biochemistry and Cell Biology, 1998, 76, 497-502.	0.9	4

148 Metabolite-specific NMR spectroscopyin vivo. , 1997, 10, 435-444.